A Novel Treatment to Selectively Harden Ti6Al4V Surfaces

Wei, Qi; Zhang, Zhenxue

Document Version
Publisher's PDF, also known as Version of record

[Link to publication on Research at Birmingham portal](#)

Article

A Novel Treatment to Selectively Harden Ti6Al4V Surfaces

Qi Wei* and Zhenxue Zhang

Read Online

ACCESS | Metrics & More | Article Recommendations

ABSTRACT: Various surface treatments have been developed on titanium and its alloy to improve their tribological properties. However, for some components, only specific surfaces need to be hardened rather than the whole surfaces. This study develops a duplex heat treatment including selective surface hardening by prepainting TiO_2 powders and thermal oxidation. It is found that the TiO_2 powder layer can be used as an oxygen reservoir for boosting diffusion treatment at temperatures of 800−900 °C. The abundance of oxygen provides high potential and accelerates the diffusion process, deeply hardening the surface case. Moreover, the duplex treatment is optimal for selectively hardened surfaces with high load-bearing capacity and much improved tribological properties. Prepainting the surfaces that need to be hardened is easy to operate and has good potential to be applied in industry.
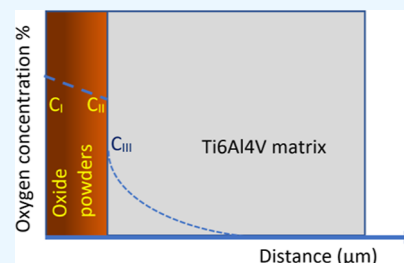
INTRODUCTION

Titanium and its alloys have been extensively used in the aeronautical, marine, and chemical industries due to their high strength, good oxidation, and corrosion resistance.[1,2] However, their poor tribological properties and low hardness restrict the applications of titanium alloys under heavy loads.[3] Various surface modifications have been worked out to improve the surface properties of titanium alloys. For example, plasma nitriding gives titanium surfaces a low friction coefficient; nevertheless, it has demerits including high treatment temperature, long treatment time, large distortion, and thin treated layers.[4−6] Thermal spraying is another technique to coat titanium alloys, but the coating density is a problem and the bond strength is low.[7] Other surface treatment methods such as shot peening, electroplating, ion implantation, PVD, and laser surface alloying are also applied.[8−10] A common problem for the above-mentioned methods is that the load-bearing capacity (LBC) of these thin modified layers is not high enough due to the soft substrate, which limits their applications.[11,12]

Over the past 50 years, numerous studies have been conducted on the oxidation of titanium alloys, which was generally regarded as a chemical problem rather than as a surface-strengthening method. Direct heat treatment at elevated temperatures (850−1000 °C) on Ti6Al4V could achieve a satisfactory surface hardening effect, but it produced a scale that severely compromised its fatigue property.[4,13] Hence, this process was not commercially feasible. Recently, a ceramic conversion treatment was developed at the University of Birmingham in which titanium alloys were heated at 600−700 °C for up to 120 h to produce an adherent oxide layer supported by a shallow diffusion zone.[14] Mishra tried to enhance the abrasive resistance of a Ti22V4Al β titanium alloy

by thermally oxidizing it at 850 °C in the air, while the void in the oxide layer was larger than expected, so it was not compact enough.[15] Furthermore, the shallow diffusion zone cannot support the oxide layer for a heavy load for long, and an oxygen boost diffusion (OBD) to produce a deep hardened case on titanium alloys was reported and successfully used.[16,17] However, the fatigue properties of the OBD-treated titanium were found to be significantly reduced due to the formation of the oxygen diffusion (OD)-hardened α case, which is particularly hard but relatively brittle.[18]

In industry, only specific surfaces need to be hardened for some components. For instance, for a titanium gear, only the tooth surfaces need to be hardened and the rest of the surface should be free from oxygen to maintain its toughness and fatigue strength. This can maximize the performance of the titanium gear in terms of high hardness and wear resistance of the articulating tooth surfaces together with high fatigue properties and high specific strength.[19,20] Therefore, how to achieve selective deep-case hardening of titanium alloys is an important task from both scientific and technological points of view. This work aims at developing a novel selective deep-case hardening technique for titanium alloys via nanoparticle prepainting and vacuum diffusion. First, we prepainted TiO_2 nanopowders on the surfaces that need to be hardened, and then we treated the samples in a vacuum furnace at elevated temperatures, allowing oxygen to diffuse into the substrate.

A

Table 1. Mechanical Properties of the Ti6Al4V Alloy (Reprinted in Part with Permission from Ref 21)

elongation at break, %	modulus of elasticity (GPa)	tensile strength (MPa)	fracture toughness (MPa $\sqrt{m}$)	hardness (Vickers)	fatigue strength (MPa)	shear modulus (GPa)
<10	106−114	896−1410	66−88	349	510	44

Finally, we did a series of tests including morphological, chemical composition analysis, and mechanical properties to figure out the optimum treatment process.

■ MATERIALS AND METHODS

Ti6Al4V (ASTM Grade 5) was used in this study, and its mechanical properties are summarized in Table 1. The as-received Ti6Al4V bar (ø25 mm) was cut into disks with a thickness of 4.5 mm. The disks were ground with SiC sandpapers gradually from 120 to 1200 grids. The TiO_2 powders were commercially sourced (7920DL TiO_2 nano-powder/nanoparticles rutile, 99.5%, 10−30 nm Sky-Spring Nanomaterials, Inc., USA). Before painting the TiO_2 powder onto the titanium surfaces, all samples were cleaned in acetone for 15 min using an ultrasonic cleaner to remove any contaminants on the surface. The TiO_2 rutile powders were physically mixed with the isopropanol solvent to obtain a TiO_2 slurry. This slurry was then painted with a flat paintbrush only to the sample surfaces to be deep-case-hardened. Once painted with TiO_2 powders, the samples were kept for more than 24 h in open, dry air to ensure that the solvents fully evaporated.

OBD was carried out in a TAV vacuum heat treatment furnace (Vacuum Furnace Engineering LTD, UK). All the samples including the selectively painted samples and the fully preoxidized ones were put into the vacuum furnace which was pumped down to 2.56×10^{-6} mbar. Then, the samples were heated at the rate of 10 °C/min to the required temperature and stayed for the preset period before cooling in the vacuum chamber until room temperature.

The selective OD (SOD) treatment of Ti6Al4V was carried out at temperatures below β transition (995 ± 20) °C ranging from 800 to 900 °C according to previous experience,[16] and the diffusion time range was chosen from 10 to 30 h to achieve a decent hardened case. The reference sample (OBD) was first oxidized at 800 °C for 25 min and then boost-diffused at 850 °C for 30 min in vacuum.[22]

An additional thermal oxidation (TO) treatment in the air (600 °C/80 h) was performed on both untreated and SOD 850/10-treated samples to compare their tribological properties. Details of the sample code and the process conditions are listed in Table 2.

The microstructures were observed under an optical microscope (VHX-5000, Keyence, Japan) and scanning electron microscope (Joel 6060, JEOL Ltd., Japan), while the elemental composition was detected by energy-dispersive X-ray spectroscopy (Oxford Instruments, UK). The phase constitution was examined by X-ray diffraction (D8 ADVANCE, Bruker, US) with Cu Kα radiation. The cross-sectional chemical composition was analyzed with a finely focused ion beam (FIB) in an FEI Quanta 3D FEG dual-beam electron microscope equipped with EDX. To measure microhardness, the indentations were carried out by an MHV-1000 micro-hardness tester (MRC Ltd-LABORATORY EQUIP-MENT, UK) with a Vickers diamond pyramidal indenter and a Carl Zeiss NU2 microscope. A nanoinstrument (NanoTest Vantage, Micro Materials, UK) was used to acquire mechanical properties such as nanohardness and Young's modulus. The

Table 2. Sample Code and Corresponding Treatment Conditions

sample code	pre-OD process	OD	TO
		T (°C)/t(h)	T (°C)/t(h)
SOD 800/15	paint TiO_2	800/15	
SOD 850/10	paint TiO_2	850/10	
SOD 850/15	paint TiO_2	850/15	
SOD 850/30	paint TiO_2	850/30	
SOD 900/15	paint TiO_2	900/15	
OBD[a]	800 °C for 25 min	850/30	
TO			600/80
SOD + TO	paint TiO_2	850/10	600/80
UNT	as received		

[a]Repetition of Dong's work[17] as a reference sample.

coefficient of friction (CoF) was acquired with a Phoenix TE79 reciprocal Friction Tester under a load of 2.5 N running for 1000 cycles. The wear resistance was assessed by a homemade machine that used an 8 mm-diameter hardened (853HV) SAE52100 ball under a load of 6 N against the test surfaces for 1020 reciprocal cycles in each test.

■ RESULTS

Surface Morphology. As shown in Figure 1b,c, the prepainted white TiO_2 powders on the Ti6Al4V sample surface turned into dark color with scattered gray areas after boost diffusion treatment in vacuum (SOD 850/30). The other half of the Ti6Al4V sample surface without prepainted powders also became gray after boost diffusion. The metallic luster of the surface became dark brown after oxidation at 800 °C for 25 min in the air (Figure 1d); after boost diffusion, the surface turned grayish (Figure 1e). These appearance changes are in agreement with the full OBD of the Ti6Al4V sample in Dong's work.[17]

Phase Constituent of SOD Samples. The residual powder was loosely bound to the sample surface. Ultrasonic cleaning was used to remove the residual powder of the sample SOD 850/30, and XRD was performed on the powders and revealed the surface. The phase analysis was performed with Match! Software (V3.0) with the crystallography open database.

As seen in Figure 2a, although there were still some rutile TiO_2 peaks, much more oxygen-deficient oxide peaks like Ti_7O_{13}, Ti_4O_7, and Ti_2O_3 were identified, and the titanium peaks were also detectable. A small number of oxides of rutile and aluminide were still identified on the surface of both painted and unpainted sides after SOD. However, the phase of α-Ti and β-Ti gradually dominated the surface (Figure 3b,c). In comparison with the standard XRD pattern of Ti6Al4V,[23] (i) the number of peaks for the β phase reduced after SOD, (ii) the peak width for the α phase was broadened, and (iii) the peak angles (2θ) shifted slightly.

Chemical Composition. As shown in Figure 3a, EDX was used to collect the elemental information in the remaining powders coated on the surface of the samples after the SOD process. The average oxygen content in the powders left on the
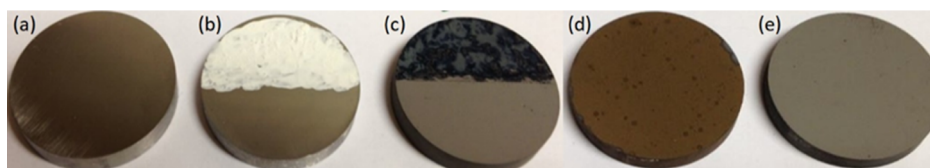
Figure 1. Sample morphology of the samples: (a) as-ground, (b) prepainted with rutile slurry, (c) after SOD 850/30 treatment, (d) preoxidation in air at 800 °C/25 min, and (e) after OBD treatment (850 °C/30 min in vacuum).
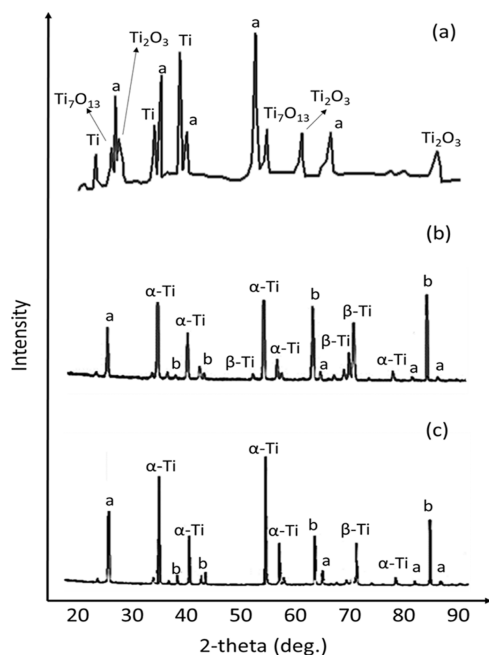

Figure 2. XRD pattern of the (a) remaining powder on SOD 850/30, (b) unpainted side of SOD 850/30, and (c) prepainted side of SOD 850/30. (a) TiO_2 (rutile) and (b) Al_2O_3.

SOD-processed samples is summarized in Figure 3b. After 10 h of boost diffusion at 850 °C, the oxygen in the remaining powder layer (Figure 3a) was about 35 at % and it reduced further with increasing diffusion time and down to 22 at % after 30 h of boost diffusion. At a given temperature, e.g., 850 °C, the oxygen content decreased with the increment of the treatment time. After 15 h of boost diffusion, the oxygen concentrations were about 34 at %, 30 at %, and 29 at % separately for samples treated at 800, 850, and 900 °C,

respectively, and the oxygen concentration decreased with increasing temperature.

As seen in Figure 4a, a cross-sectional trench was cut by FIB, and a line scan was performed along the powder coating and the Ti6Al4V sample by EDX. "A" in Figure 4b is part of the OD zone close to the interface; a higher oxygen plateau was found in the near-surface region between the two lines as displayed in Figure 4c. Meanwhile, the oxygen content in the powders increased gradually from the interface to the surface of the powder coating, indicating that oxygen was released from TiO_2 powder and diffused into the titanium sample.

Layer Structure and Hardness Depth Profiles. The as-received Ti6Al4V material is an $\alpha + \beta$ mixture with the elongated β-phase evenly distributed in the equiaxed α-phase matrix. After SOD treatment, a hardened layer caused by OD can be easily distinguished under optical micrography with a brightened near-surface zone as displayed in Figure 5a for a typical sample SOD850/30, and the thickness of this layer is about 200 μm. The cross-sectional microstructure observed by SEM suggested that the α-phase was enlarged with less β-phase in the near-surface region as seen in Figure 5b, and the light-colored β-phase increased with the depth gradually. Further observation of the boundary part of the painted and unpainted zone after SOD indicated that the painted side is clearly darker than the unpainted side under the optical microscope as shown in Figure 5c.

Hardness Depth Profiles. The hardness values along the depth are plotted in Figure 6. Generally speaking, the hardness values decreased from the surface to the substrate depending on the treatment temperature and time. For example, the surface hardness of the SOD 850/30 sample (Figure 6a) was 849.2HV$_{0.025}$ and the hardened zone reached approximately 500 μm. For SOD 850/15 and SOD 850/10, the surface hardness and affected zone became 645.9HV$_{0.025}$ and 250 μm and 623.7HV$_{0.025}$ and 200 μm, respectively. Accordingly, a higher temperature led to higher hardness and a deeper
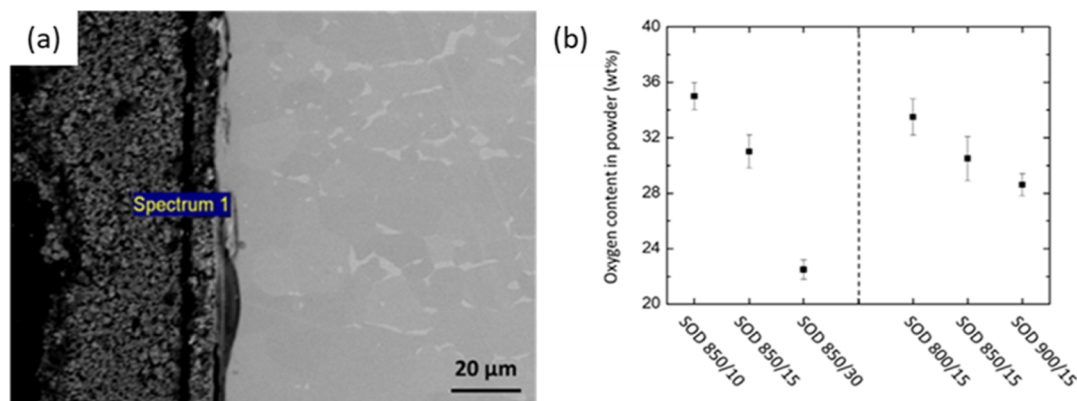

Figure 3. (a) SEM image of a SOD sample, indicating the spectral point for EDX analysis. (b) The oxygen content of the powders was detected by EDX in SOD samples.
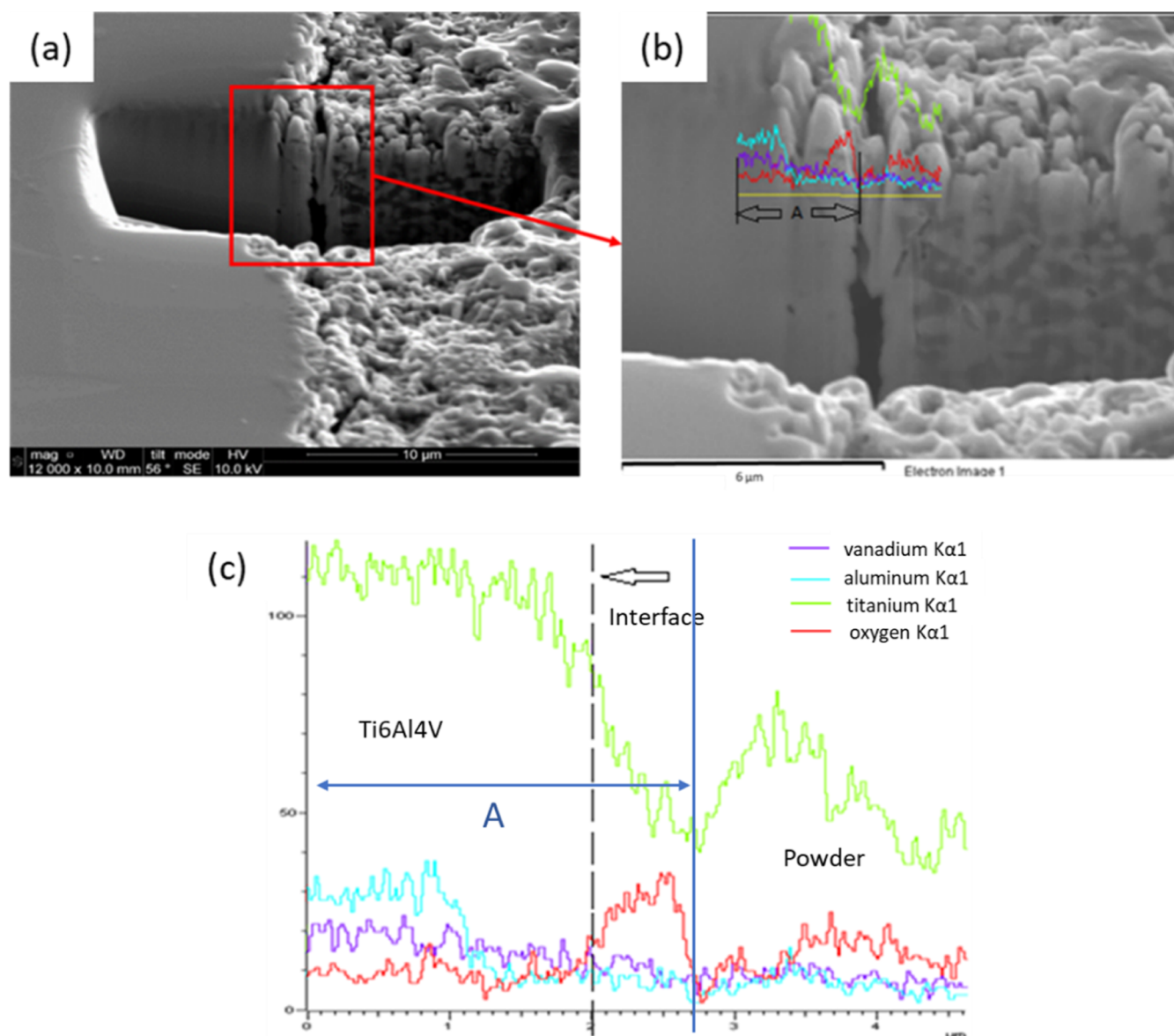
Figure 4. FIB-SEM image and EDX analysis for the SOD 850/15 sample. (a) FIB cut trench crossing the interface between the powder layer and the Ti6Al4V sample. (b) EDX line scan zone. (c) Element distributions along the interface.

affected zone as shown in Figure 6b. In comparison to the OBD reference sample (Figure 7), at the same diffusion temperature and time, the hardness values for the SOD sample were higher with a deeper hardening zone which might be due to a more abundant oxygen resource.

Nanohardness was also measured on a smaller scale (20 mN), and the distribution of nanohardness vs the depth was also plotted as shown in Figure 8, which has a similar trend as the microhardness results. Young's modulus fluctuated between 125 and 160 GPa, indicating that the extraneous oxygen did not result in phase change.

Oxygen is an α stabilizer, and the introduction of oxygen induces the transfer of the β phase to the α phase, which leads to a clear brighter near-surface main diffusion region as shown in Figure 9a. Meanwhile, oxygen is also a solid solute strengthener, higher content of oxygen in the α-phase boosts the hardness of the matrix. Although in the relative diffusion zone, there is not much change in the α and β phases, the interstitial oxygen can also improve the hardness. Accordingly,

the hardened layer thickness included both these zones and they were measured and are summarized in Figure 9b,c.

Load-Bearing Capacity. The surface hardness of the untreated, TO, SOD 850/10, and SOD + TO samples was measured under different loads of 10, 25, 50, 100, 200, 300, 500, and 1000 g to evaluate the static LBC of the surface. As seen in Figure 10, the SOD sample had a relatively lower hardness than TO and SOD + TO samples under a 10 g load and gradually decreased with the increase of the load until 50 g. When the applied load exceeded 50 g, the measured hardness decreased sharply from 50 to 100 g and then slowly till 300 g to substrate hardness. Both the TO and SOD + TO samples achieved high hardness values under the loads of 10 and 50 g, but upon further increasing the load, only the SOD + TO sample retained a high level until a load of 200 g, indicating that the SOD zone boosts the LBC of the thin oxide layer.

Tribological Properties. As shown in Figure 11, when the tungsten carbide ball slid on the surface of Ti6Al4V, a higher
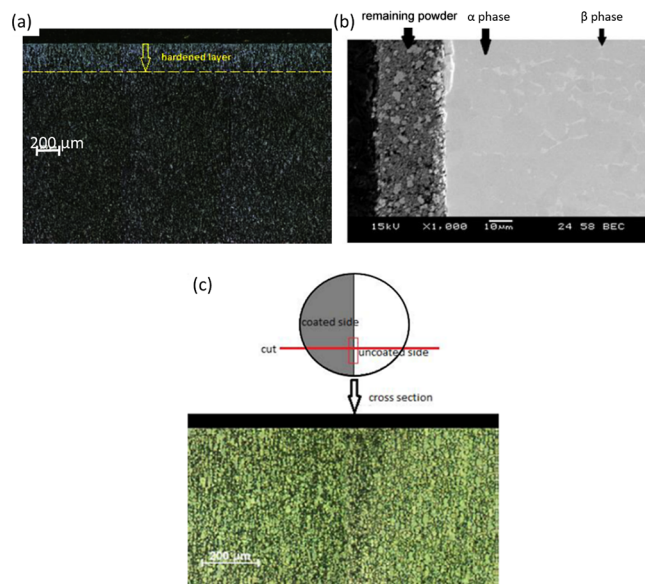
Figure 5. Cross-sectional microstructure viewed under an (a) optical microscope for SOD 850/30 and (b) SEM for SOD 900/15. (c) Boundary zone under an optical microscope observed for SOD 850/15.
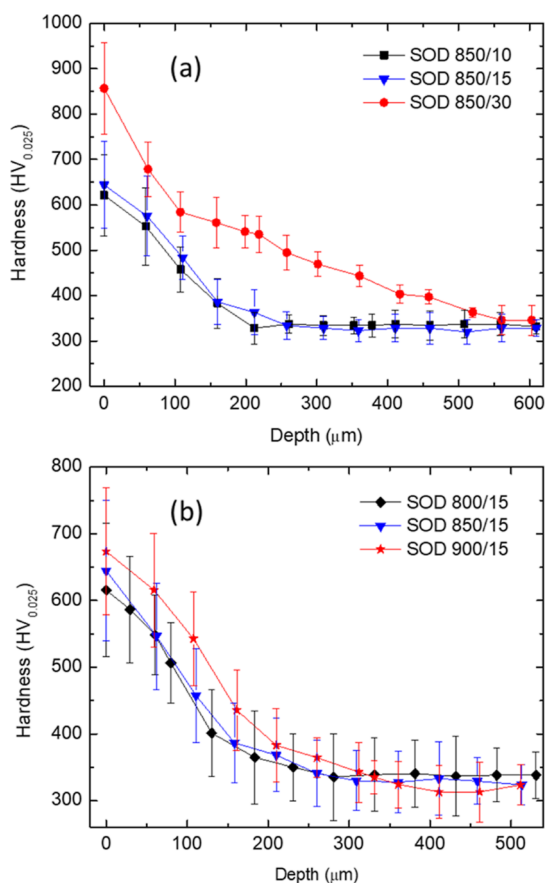

Figure 6. Microhardness profile of SOD samples: (a) 850 °C for different times and (b) 15 h at different temperatures.

and unstable CoF fluctuated between 0.2 and 0.5 in the whole reciprocal process. The CoF started low for the TO surface, and it increased steadily with the increment of the tribotest till 0.45 in the end which might be attributed to the thin oxide
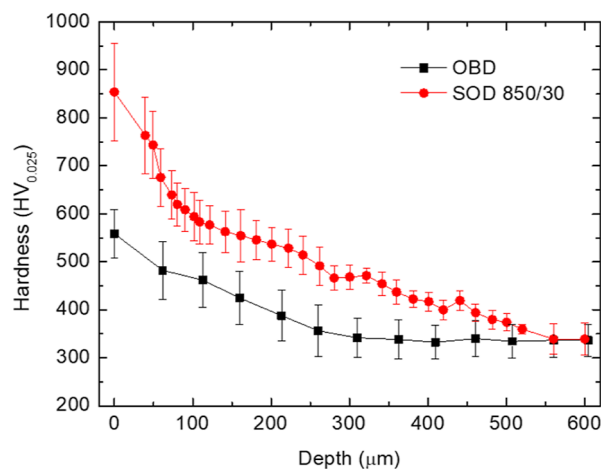

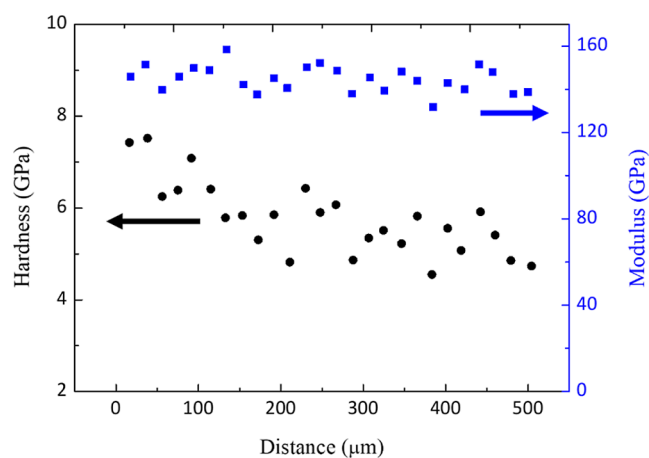**Figure 7.** Hardness profile for the sample: OBD and SOD 850/30.

Figure 8. Nanohardness profile and the corresponding elastic modulus in SOD 850/15.

layer (1−2 μm) worn through at about 700 cycles.[17,24] For the SOD sample, the CoF was higher in the first part of the test which might be caused by the remaining powders on the surface, and it slightly reduced after half of the test cycles, and the change in the CoF was in a narrow range. The sample SOD + TO had a low CoF in the beginning and increased slightly but remained low and relatively stable under 0.2 in the whole process. The duplex-treated SOD + TO surface outperformed all the other samples mainly due to the deep hardened case which could provide strong support to the top oxide layer, as evidenced by the LBC shown in Figure 11.

The wear resistance of different surfaces under reciprocal sliding conditions was assessed by using an 8 mm hardened (853HV) SAE52100 ball under a load of 6 N for 1020 cycles. The wear scar was scanned by a 2D profilometer, and the results are shown in Figure 12. The wear scar depth and wear area loss for the SOD + TO sample was only 1 μm and 85.09 μm^2, while for SOD and TO samples, these values increased to 30 μm and 15,018 μm^2 and 40 μm and 20,978 μm^2, respectively. The wear tracks formed on all the tested surfaces were observed under SEM and are displayed in Figure 13. A deep and wide scuffed track was formed on the surface of the untreated samples, while similar scuffed narrower tracks were formed on the surface of the SOD and TO samples. However, a much narrower and relatively smooth scar appeared on the
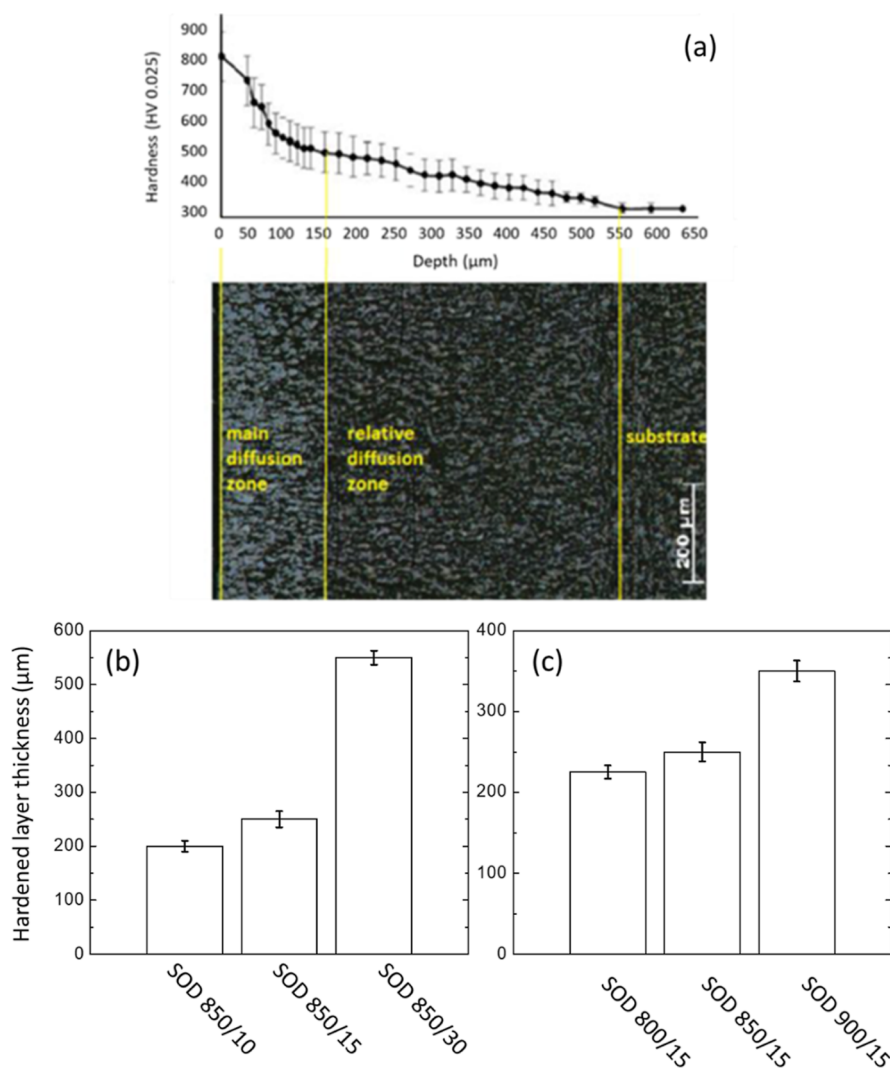
Figure 9. (a) Hardness profile and the corresponding microstructure under an optical microscope for SOD 850/30. Hardened layer thickness for samples after different SOD processes, (b) SOD 850 with different times, and (c) SOD for 15 h at different temperatures.
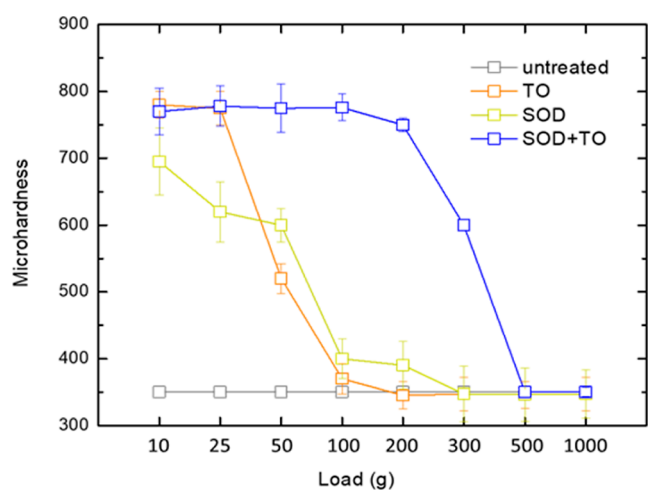

Figure 10. Hardness under different loads (the average hardness value of the untreated one is used as a standard).

Figure 11. CoF changes with the test cycles of four samples.

DISCUSSION

Titanium has a strong affinity to oxygen; when titanium alloys are exposed to air at higher temperatures, oxygen molecules are adsorbed and dissociated into oxygen atoms which react with the activated titanium surfaces to form a titanium oxide layer. Meanwhile, some oxygen diffuses through the oxide into the matrix to form a diffusion zone under the oxide layer. Ceramic conversion treatment was normally carried out at 600−700 °C to generate a 2−3 μm compact oxide layer with a diffusion

SOD + TO surface with little scratches in the track which indicated strong wear resistance.

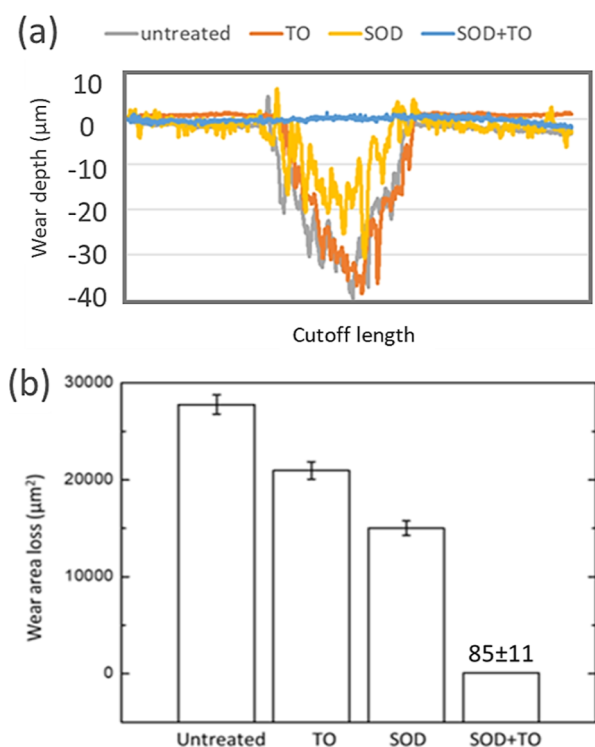**Figure 12.** (a) 2D wear scars and (b) wear area loss for four samples with different surface treatment conditions.
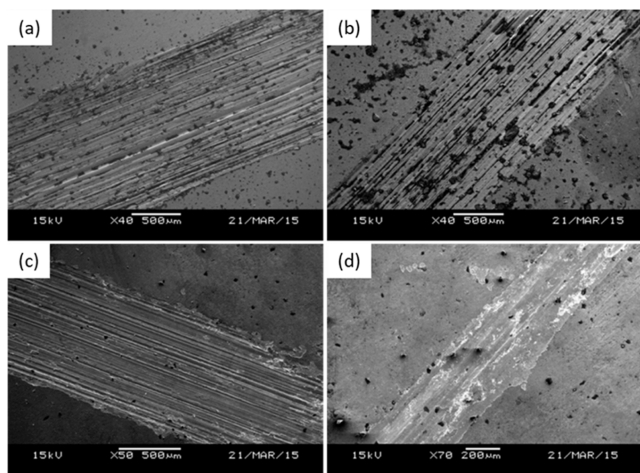

Figure 13. Wear scar under SEM for samples of (a) untreated, (b) SOD, (c) TO, and (d) SOD + TO.

zone of 30−50 μm. However, this thin diffusion zone is normally not enough to support a higher load which necessitates the application of boost diffusion treatment, which can generate a diffusion zone of up to 300 μm. In practical applications, mechanical parts like gear may only need to selectively harden the surface. Therefore, in this work, we prepainted nanosized TiO_2 powders on the selected surface of the Ti6Al4V sample and then subjected the samples to boost diffusion in vacuum at temperatures between 800 and 900 °C.

As shown in Figure 1, after the SOD process, the white rutile TiO_2 powders turned into darker color which were oxygen-deficient oxides like Ti_7O_{13} and Ti_2O_3 (Figure 2), in which the oxygen content was lower than the stoichiometry of TiO_2.[25] If these remaining products are represented by Ti_xO_y, the reaction at the powder−metal interface can be written as

$$TiO_2(s) + Ti \rightarrow Ti_xO_y + O \tag{1}$$

This reaction resulted in the absorption and diffusion of oxygen in the titanium alloy matrix. The initial oxygen concentration of C_I in the oxide decreased to C_{II} near the interface (Figure 14). Oxygen concentration (C_{III}) started to
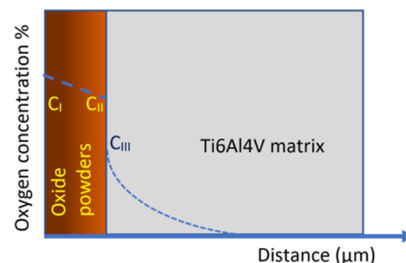

Figure 14. OD model for parabolic oxidation.

build up near the interface in the matrix, and a gradient was formed which helped the oxygen atoms diffuse into the matrix as shown in Figures 4c and 5. As the oxides dissociated at the interface area, the oxygen-deficient Ti_xO_y could also combine with Ti to release further oxygen and titanium as shown in eq 2

$$Ti_xO_y + Ti \rightarrow Ti_{x1}O_{y1} + Ti + O \tag{2}$$
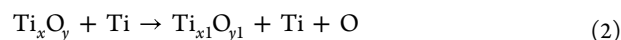
The free oxygen will move to the substrate, while the released titanium can further react with TiO_2 to liberate more oxygen, and thus, a gradient will also form in the painted oxide layer as shown in Figure 14.

Another reaction can also occur as shown in eq 3

$$TiO_2 \rightarrow Ti_xO_y + O \tag{3}$$

However, this mechanism may not dominate the process as the partial pressure (about 10^{-4} mbar) in the furnace is higher than the dissociated pressure of oxygen which is about 10^{-31} mbar at 850 °C.[26]

The hardness of the Ti6Al4V alloy is proportional to the oxygen concentration;[26] from the trend of the hardness profiles in Figures 6−8, the OD generally follows Fick's law.

As seen in Figure 7, the hardness in the prepainted sample (SOD) was higher than that in the preoxidation one (OBD), although they were both boost-diffused at the same temperature and time which might be due to a low abundance of oxygen. The scale formed on the surface of OBD was thin (about 3−4 μm); however, the painted oxide layer on SOD was several millimeters thick. As a result, the oxygen concentration in the metal at the oxide/metal interface C_{III} became lower when the thin oxide layer disappeared from the preoxidized sample OBD, resulting in a relatively low hardness profile.[27] However, in the prepainted sample, the abundant oxygen supply from the thick oxide powder layer guaranteed stable oxygen concentration at the oxide/metal interface which led to a higher hardness profile than that of the preoxidized one as seen in Figure 7.

It is known that the SOD process can improve the hardness of titanium alloys by solid solute strengthening, but it does not change the poor tribological properties because the essence of metal is still titanium.[28] In other words, no new phase formed during the SOD process, which might still lead to adhesion to the counterpart. However, with another TO process, a ceramic rutile layer was covered on the surface, which decreased the CoF greatly because it impeded the contact of titanium and the

rubbing material, as evidenced in Figure 11. Both samples TO and TO + SOD had lower CoF at the beginning of the tribotest. However, the CoF for sample TO increased gradually with the test time, and it was about the same as that for the untreated sample after about 500 cycles when the oxide layer was worn through, which might be due to the soft substrate not being able to support the ceramic layer effectively.[29] Once the oxide layer broke, the hard oxide debris together with the adhesive titanium could increase the friction and accelerate the wear. Because of the lack of strong support, the LBC of TO was not as good as that of SOD + TO (Figure 10).

In brief, duplex treatment (SOD + TO) significantly improved the LBC and the tribological properties of the Ti6Al4V material in comparison to the other treatments. With the support of a deep hardened case produced during SOD, the ceramic TiO_2 layer can bear a heavy load in both static and dynamic conditions.

CONCLUSIONS

Prepainting TiO_2 nanopowders on the Ti6Al4V surface acted as a reservoir of oxygen in the vacuum boost diffusion process to achieve selective surface hardening, and the following conclusions can be drawn:

The prepainted powder served as an oxygen reservoir for boost diffusion at 800−900 °C, and TiO_2 decomposed to oxygen-deficient oxides such as Ti_7O_{13}, Ti_4O_7, and Ti_2O_3. Higher temperatures and longer treatment times introduced more oxygen into the Ti6Al4V substrate.

The oxygen content reduced gradually from the interface into the substrate. The higher oxygen content in the near-interface zone produced an α-phase-predominated diffusion zone which has higher hardness due to the solid solute strengthening effect of oxygen. In the major diffusion zone, although the α and β phases coexisted, the hardness also improved. Therefore, a deeper OBD zone was formed. For example, the hardened region was about 500 μm after SOD at 850 °C for 30 h.

The SOD process produced a better hardening effect than the conventional OBD method due to the abundant supply of oxygen. The SOD + TO duplex-treated selectively hardened surfaces had high LBC, lower CoF, and higher wear resistance.

AUTHOR INFORMATION

Corresponding Author

Qi Wei − Aviation Key Laboratory of Science and Technology on Advanced Surface Engineering, AVIC Manufacturing Technology Institute, Beijing 100024, China; School of Metallurgy and Materials, University of Birmingham, Birmingham B152TT, U.K.; ● orcid.org/0000-0002-4711-4668; Email: weiq057@avic.com

Author

Zhenxue Zhang − School of Metallurgy and Materials, University of Birmingham, Birmingham B152TT, U.K.

Complete contact information is available at:
https://pubs.acs.org/10.1021/acsomega.3c02778

Notes

The authors declare no competing financial interest.

REFERENCES

(1) Nastac, L.; Gungor, M. N.; Ucok, I.; Klug, K. L.; Tack, W. T. Advances in investment casting of Ti−6Al−4V alloy: a review. Int. J. Cast Met. Res. 2013, 19, 73−93.

(2) Chen, W.; Zhang, D.; Wang, E.; Yan, F.; Xiang, L.; Xie, Z. Corrosion Degradation Behaviors of Ti6Al4V Alloys in Simulated Marine Environments. Coatings 2022, 12, 1028.

(3) Li, X.; Yue, W.; Huang, F.; Kang, J.; Zhu, L.; Tian, B. Tribological behaviour of textured titanium under abrasive wear. Surf. Eng. 2018, 35, 378−386.

(4) Wang, Z.-M.; Jia, Y.-F.; Zhang, X.-C.; Fu, Y.; Zhang, C.-C.; Tu, S.-T. Effects of Different Mechanical Surface Enhancement Techniques on Surface Integrity and Fatigue Properties of Ti-6Al-4V: A Review. Crit. Rev. Solid State Mater. Sci. 2019, 44, 445−469.

(5) Yetim, A. F.; Kovacı, H.; Uzun, Y.; Tekdir, H.; Çelik, A. A comprehensive study on the fatigue properties of duplex surface treated Ti6Al4V by plasma nitriding and DLC coating. Surf. Coat. Technol. 2023, 458, 129367.

(6) Ongtrakulkij, G.; Kajornchaiyakul, J.; Kondoh, K.; Khantachawana, A. Investigation of Microstructure, Residual Stress, and Hardness of Ti-6Al-4V after Plasma Nitriding Process with Different Times and Temperatures. Coatings 2022, 12, 1932.

(7) Weicheng, K.; Kangmei, L.; Jun, H. Effects of laser power on microstructure and friction−wear performances of direct energy deposited ZrO2−8%Y2O3−NiCoCrAl coatings on Ti6Al4V alloy. Opt. Laser Technol. 2021, 142, 107214.

(8) Luo, X.; Dang, N.; Wang, X. The effect of laser shock peening, shot peening and their combination on the microstructure and fatigue properties of Ti-6Al-4V titanium alloy. Int. J. Fatigue 2021, 153, 106465.

(9) Herrera-Jimenez, E. J.; Bousser, E.; Schmitt, T.; Klemberg-Sapieha, J. E.; Martinu, L. Effect of plasma interface treatment on the microstructure, residual stress profile, and mechanical properties of PVD TiN coatings on Ti-6Al-4V substrates. Surf. Coat. Technol. 2021, 413, 127058.

(10) Vazirgiantzikis, I.; George, S. L.; Pichon, L. Surface character-isation and silver release from Ti-6Al-4V and anodic TiO2 after surface modification by ion implantation. Surf. Coat. Technol. 2022, 433, 128115.

(11) Xiao, H.; Liu, X.; Lu, Q.; Hu, T.; Hong, Y.; Li, C.; Zhong, R.; Chen, W. Promoted low-temperature plasma nitriding for improving wear performance of arc-deposited ceramic coatings on Ti6Al4V alloy via shot peening pretreatment. J. Mater. Res. Technol. 2022, 19, 2981−2990.

(12) Shukla, A. K.; Balasubramaniam, R.; Bhargava, S. Properties of passive film formed on CP titanium, Ti−6Al−4V and Ti−13.4Al−29Nb alloys in simulated human body conditions. Intermetallics 2005, 13, 631−637.

(13) García, I.; de la Fuente, J.; de Damborenea, J. J. (Ti,Al)/(Ti,Al)N coatings produced by laser surface alloying. Mater. Lett. 2002, 53, 44−51.

(14) DongLi, H. X. Ceramic conversion treatment of titanium-based materials. Surface engineering of light alloys; Woodhead Publishing Limited, 2010; pp 477−499.

(15) Mishra, A. K.; Davidson, J. A.; Poggie, R. A. Diffusion hardening—a new surface hardening process for titanium alloys. Surf. Modif. Technol. VII, Proc. Int. Conf., 7th 1994, 212, 453−471.

(16) Zhang, Z. X.; Dong, H.; Bell, T.; Xu, B. The effect of treatment condition on boost diffusion of thermally oxidised titanium alloy. J. Alloys Compd. 2007, 431, 93−99.

(17) Dong, H.; Li, X. Oxygen boost diffusion for the deep-case hardening of titanium alloys. Mater. Sci. Eng., A 2000, 280, 303−310.

(18) Hornberger, H.; Randow, C.; Fleck, C. Fatigue and surface structure of titanium after oxygen diffusion hardening. *Mater. Sci. Eng., A* **2015**, *630*, 51−57.

(19) Ignatijev, A.; Nečemer, B.; Kramberger, J.; Glodež, S. Fatigue crack initiation and propagation in a PM-gear tooth root. *Eng. Failure Anal.* **2022**, *138*, 106355.

(20) Zhao, J.; Hou, L.; Li, Z.; Zhang, H.; Zhu, R. Prediction of tribological and dynamical behaviors of spur gear pair considering tooth root crack. *Eng. Failure Anal.* **2022**, *135*, 106145.

(21) ASTM International. F1108-97a, *Standard Specification for Ti6Al4V Alloy Castings for Surgical Implants (UNS R56406)*, ASTM International, West Conshohocken, PA, 1997, www.astm.org.

(22) Dong, H. *Surface Engineering of Light Alloys: Aluminium, Magnesium and Titanium Alloys*, 1st ed.; Elsevier: Amsterdam, Netherlands, 2010; pp. 277-281.

(23) Xie, B.; Fan, Y.; Zhao, S. Characterization of Ti6Al4V powders produced by different methods for selective laser melting. *Mater. Res. Express* **2021**, *8*, 076510.

(24) Aniołek, K.; Kupka, M.; Barylski, A. Characteristics of the tribological properties of oxide layers obtained via thermal oxidation on titanium Grade 2. *Proc. Inst. Mech. Eng., Part J* **2018**, *233*, 125−138.

(25) Nowotny, J.; BAK, T.; Nowotny, M. K.; Sheppard, L. R. Chemical Diffusion in Metal Oxides. Example of TiO_2. *Ionics* **2006**, *12*, 227−243.

(26) Zhang, Z. *The Effect of Treatment Condition on Boost Diffusion of Thermally Oxidised Titanium Alloy PhD thesis*; University of Birmingham: United Kingdom, 2007.

(27) Vaché, N.; Cadoret, Y.; Dod, B.; Monceau, D. Modeling the oxidation kinetics of titanium alloys: Review, method and application to Ti-64 and Ti-6242s alloys. *Corros. Sci.* **2021**, *178*, 109041.

(28) Jiang, Y.; Mao, H.; Xiaowei, W.; Lu, Y.; Gong, J. Effect of oxygen boost diffusion treatment on the mechanical properties of Ti-6Al-4V alloy. *Surf. Interfaces* **2021**, *25*, 101248.

(29) Zhang, Z. X.; Dong, H.; Bell, T.; Xu, B. S. The effect of deep-case oxygen hardening on the tribological behaviour of a-C:H DLC coatings on Ti6Al4V alloy. *J. Alloys Compd.* **2008**, *464*, 519−525.